Acta Cryst. (1993). A**49**, 750–755

Edge Contributions to the Kirste–Porod Formula: the Spherical Segment Case

BY S. CICCARIELLO

Dipartimento di Fisica 'G. Galilei' and INFM, via Marzolo 8, *I*-35131 *Padova, Italy*

(*Received* 18 *January* 1993; *accepted* 26 *March* 1993)

Abstract

The closed-form expression of $\gamma''_W(\mathbf{r})$, the second partial r derivative of the wide-angle correlation function of a monodisperse dilute system of particles shaped as spherical segments, is worked out. From this result, the explicit value, at $r = 0$, of the third derivative of the small-angle correlation function is obtained. The value differs from that obtained by the Kirste–Porod formula by a *positive* contribution, owing to the circular edge.

I. Introduction

The main assumption of small-angle X-ray scattering (SAXS) theory is that the electron density $n(\mathbf{r})$ of the sample can be approximated by a discrete-valued function $n_D(\mathbf{r})$, which, for greater simplicity, will be assumed to be two valued in the following (see, for example, Ciccariello, Goodisman & Brumberger, 1988). From this assumption, it follows that the sample comprises two phases [*i.e.* the regions V_1 and V_2, where $n_D(\mathbf{r})$ is equal to n_1 and n_2, respectively] and that the phases are separated by a surface, referred to as the sample interface. Some of the geometrical parameters of the interface can be obtained from the coefficients $\gamma'(0)$ and $\gamma'''(0)$ present in the asymptotic expansion of the SAXS intensity $I(h)$ (see, for example, Porod, 1982):*

$$i(h) \equiv I(h)/V\langle\eta^2\rangle \simeq -[8\pi\gamma'(0)/h^4] + [16\pi\gamma'''(0)/h^6] + \ldots . \quad (1)$$

In fact, Porod (1951) and Debye, Anderson & Brumberger (1957) found that $\gamma'(0) = -S \times (4V\Phi_1\Phi_2)^{-1}$, where S is the area of the interface, while Kirste & Porod (1962) have shown that

$$\gamma'''(0) = \mathscr{K}/(4V\Phi_1\Phi_2) \quad (2)$$

* The meanings of the symbols present in (1), (2) and (4) are as follows: $h = (4\pi/\lambda)\sin(\theta/2)$ is the momentum transferred to a photon, of wavelength λ, which elastically scatters by the angle θ; V is the volume of the sample; $\langle\eta^2\rangle$ is the average of the squared electron-density fluctuation, defined as $\eta(\mathbf{r}) = n_D(\mathbf{r}) - \langle n\rangle$, with $\langle n\rangle$ denoting the average electron density of the sample; $n_D(\mathbf{r}) \equiv n_1\rho_1(\mathbf{r}) + n_2\rho_2(\mathbf{r})$, where $\rho_i(\mathbf{r}) = 1$ when $\mathbf{r}$ falls inside the region V_i and $\rho_i = 0$ elsewhere; $\Phi_i = V_i/V$ is the volume fraction of the ith phase; $\hat{\omega}$ is a unit vector.

$$\mathscr{K} \equiv 1/(16)\int_S dS[(3/R_m^2) + (2/R_mR_M) + (3/R_M^2)], \quad (3)$$

where R_m and R_M denote the principal-curvature radii (Stoker, 1989) of the interface. It should be remembered that $\gamma'(0)$ and $\gamma'''(0)$ denote the values, at $r = 0$, of the first and third derivatives, respectively, of the SAXS correlation function, defined as

$$\gamma(r) = (4\pi V\langle\eta^2\rangle)^{-1}\int d\hat{\omega}\int_V dv_1\eta(\mathbf{r}_1)\eta(\mathbf{r}_1 + r\hat{\omega}). \quad (4)$$

[The first integral on the right-hand side (r.h.s.) of (4) is performed over all directions of $\hat{\omega}$.] Equation (3) requires that R_m and R_M exist and differ from zero at each point of the interface. Therefore, interfaces must be assumed 'smooth' for (3) to make sense. On the other hand, for many samples, the best $n_D(\mathbf{r})$ choice might require that the interface have some regions of negligible thickness, where the minima of the absolute values of the principle-curvature radii be smaller than the highest spatial resolution attainable in SAXS experiments. In these cases, description of the interfaces as surfaces with sharp edges appears more accurate. For the same reason, sharp corners and contact points might also exist. Thus, there is the problem of determining the values of $\gamma'''(0)$ for interfaces with the aforesaid singularities. In general, the latter can be expected to give rise to a contribution $\mathscr{S}$, which, added to $\mathscr{K}$, yields the exact $\gamma'''(0)$ value according to the relation

$$4V\gamma'''(0) = \mathscr{S} + \mathscr{K}. \quad (5)$$

$4V\gamma'''(0)$, $\mathscr{K}$ and $\mathscr{S}$ will be referred to henceforth as the 'roundness', 'curvosity' and 'sharpness', respectively, of the interface. The first denomination follows from the fact that $-V\gamma'''(0)$ is the angular average of the so-called rotundity parameter (Wilson, 1971), first introduced by Mitra (1964) in wide-angle X-ray scattering (WAXS) theory (see below). The second follows from (3), which explicity relates $\mathscr{K}$ to the interface curvature radii. The third makes the origin of contribution $\mathscr{S}$ evident. The determination of $\mathscr{K}$, in principle, can be carried out using (3) when the interface shape is known. However, the determination of the interface roundness, according to (5), requires that of the sharpness. The problem of determining the surface sharpness was

ISSN 0108-7673

tackled first by Sobry, Ledent & Fontaine (1991) (these authors called this quantity the 'angulosity'). They analyzed the case of particles shaped as right prisms and found that, while the linear edges (between planar facets) have zero sharpness, corners have non-null sharpness. The latter expression has been explicity worked out for the case of a corner where three edges meet with two of the three angles formed by the meeting edges equal to $\pi/2$. Moreover, these authors pointed out that the roundness of a right-circular cylinder, obtained from the relevant correlation function evaluated by Méring & Tchoubar (1968), is equal to the curvosity. Thus, similar to the case of linear edges, the circular edges of right-circular cylinders do not contribute to the sharpness. However, this conclusion is in no way general. In fact, it has been recently shown (Ciccariello, 1993) that the sharpness of the edges of a truncated circular right cone is

$$\mathscr{S} = -2\pi\tan^2(\alpha) = -\pi[\cot^2(\beta)+\cot^2(\pi-\beta)], \quad (6)$$

where α is (half) the opening angle of the truncated circular right cone, while $\beta = \pi/2 - \alpha$ and $\pi - \beta$ are the dihedral angles along the two circular edges of the truncated circular right cone. Result (6) shows that $\mathscr{S} = 0$ only when the dihedral angles are equal to $\pi/2$. Moreover, similar to the result obtained by Sobry *et al.* (1991) for the corners, the sharpness resulting from (6) is always nonpositive. Whenever this property, *i.e.* $\mathscr{S} \leq 0$, is generally true whatever the Gaussian curvatures of the intersecting surfaces, $\mathscr{S}$ will always be an upper bound of the interface roundness and this result could be of some practical relevance. Unfortunately, it is not simple to obtain the general sharpness expression. Nevertheless, it can be shown that the aforesaid conjecture is not true by explicity evaluating the sharpness of the interface relevant to a monodisperse and very dilute sample of particles shaped as spherical segments (see Fig. 1). This shape is the simplest one where the circular edge results from the intersection of two surfaces of which at least one has a Gaussian curvature different from zero.

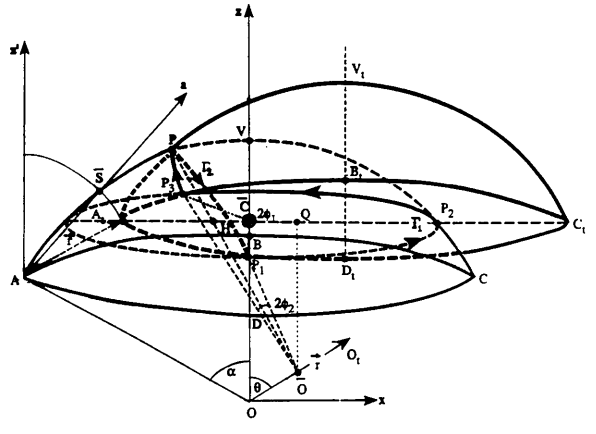

Fig. 1. A typical configuration of the set intersection of the two spherical segments; $ABCDV$ and $A_1B_1C_1D_1V_1$. The latter was obtained by translating the former by $\mathbf{r}$. The intersection curve is $\Gamma \equiv \Gamma_1 \cup \Gamma_2$, where Γ_1 is the horizontal arc $P_1P_2P_3$ and Γ_2 is the arc P_3PP_1.

This paper is devoted to the derivation of this result according to the following plan. First, §II reports the evaluation of the WAXS correlation function relevant to the aforesaid sample. It should be remembered that the WAXS correlation function, defined as

$$\gamma_W(r\hat{\boldsymbol{\omega}}) \equiv V_f^{-1}\int_V \rho_f(\mathbf{r}_1)\rho_f(\mathbf{r}_1 + r\hat{\boldsymbol{\omega}})\,\mathrm{d}v_1, \quad (7)$$

is the one-dimensional Fourier transform of the peak profile $I_{\hat{\omega}}(h)$ around reflection $\hat{\boldsymbol{\omega}}$ (Wilson, 1949).* Recalling that liquid particles on a solid surface, which are in thermodynamical equilibrium with the vapor phase, have the shape of spherical segments (Rowlinson & Widom, 1982), we can see that it is likely that the metallic particles, growing on the support of metallic catalysts by a heat treatment of the latter (Brumberger, Goodisman & Ramaya, 1990), also have the shape of spherical segments, because the physical mechanism governing the phase separation is, to a first approximation, the same. Thus, on the one hand, the determination of the peak profiles of a collection of spherical segments could be practically relevant, whenever the monodispersity condition is approximately met. On the other hand, the SAXS and the WAXS correlation functions are related by (Ciccariello, 1993)

$$\gamma(r) = -\Phi_1/\Phi_2 + (1/4\pi\Phi_2)\int \mathrm{d}\hat{\boldsymbol{\omega}}\,\gamma_W(r\hat{\boldsymbol{\omega}}), \quad (8)$$

so that, leaving aside the first constant term on the r.h.s. of (8), the former correlation function is the angular average of the latter multiplied by $1/\Phi_2$. (Note that the index 1 has been assigned to the phase formed by the particles.) Actually, when the sample is very dilute, $\Phi_2 \simeq 1$ and $\Phi_1 \simeq 0$ and $\gamma(r)$ is simply the angular average of $\gamma_W(r\hat{\boldsymbol{\omega}})$. In this way, after having determined $\gamma_W(r\hat{\boldsymbol{\omega}})$, it is possible to evaluate $\gamma''_W(r\hat{\boldsymbol{\omega}})$ [the third partial derivative of $\gamma_W(r\hat{\boldsymbol{\omega}})$ with respect to r] and its limit value as $r \to 0$. The angular average of the derivative value, denoted by $\gamma'''\boldsymbol{\omega}(0)$, with respect to all possible directions of $\hat{\boldsymbol{\omega}}$, yields $\gamma'''(0^+)$, which is proportional to the sample roundness. On the other hand, the sample curvosity can be obtained from (3) and the sharpness of the sample

* $\rho_f(\mathbf{r})$ is defined as equal to one when the tip of vector $\mathbf{r}$ falls inside one of the sample particles and equal to zero elsewhere. Thus, $\rho_f(\mathbf{r})$ coincides either with $\rho_1(\mathbf{r})$ or with $\rho_2(\mathbf{r})$, defined in the footnote to (1). V_f is the sample volume occupied by the particles and $\hat{\boldsymbol{\omega}}$ specifies the reflection direction.

follows immediately from (5). This task is performed explicitly in § III.*

II. Second-derivative expression

When the sample is very dilute and is made up of equal particles, the sample WAXS correlation function coincides with the WAXS correlation function of a single particle given by

$$\gamma_W(r\hat{\boldsymbol{\omega}}) \equiv V_p^{-1}\int_V \rho_p(\mathbf{r}_1)\rho_p(\mathbf{r}_1 + r\hat{\boldsymbol{\omega}})\,\mathrm{d}v_1, \tag{9}$$

where V_p and $\rho_p(\mathbf{r})$ refer to the volume and to the characteristic set function, respectively, of a single particle. Thus, for the particle shape shown in Fig. 1, $\rho_p(\mathbf{r}_1)$ turns out to be equal to one only when $\mathbf{r}_1$ fulfills the inequalities

$$0 \le \varphi_1 < 2\pi, \tag{10a}$$

$$0 \le \theta_1 < \alpha, \tag{10b}$$

$$\max(0, \cos\alpha) \le r_1 \le 1, \tag{10c}$$

where r_1, θ_1 and φ_1 are the polar coordinates of vector $\mathbf{r}_1 \equiv (x_1, y_1, z_1)$ with respect to the coordinate system shown in Fig. 1. Note that the unit length has been taken equal to the spherical-segment radius and that (10*c*) follows from the hypothesis that the spherical-segment opening angle obeys

$$0 \le \alpha \le \pi/2. \tag{11}$$

The integral on the r.h.s. of (9) measures the volume of the region $A_tP_3P_2P_1V$ shared by the given (or fixed) spherical segment $ABCDV$ and by the spherical segment $A_tB_tC_tD_tV_t$ obtained by translating the former by $\mathbf{r} = r\hat{\boldsymbol{\omega}}$, with $\hat{\boldsymbol{\omega}} \equiv (\cos\varphi\sin\theta, \sin\varphi\sin\theta, \cos\theta)$. It is geometrically evident that $\gamma_W(\mathbf{r})$ does not depend on φ, the longitudinal angle of $\mathbf{r}$. Therefore, $\gamma_W(\mathbf{r})$ will be written simply as $\gamma(r, \theta)$. (The omission of the index W is justified by the fact that no confusion is possible with the SAXS correlation function because the latter depends on r only.) The further symmetry $\gamma_W(\mathbf{r}) = \gamma_W(-\mathbf{r})$ implies that

$$\gamma(r, \theta) = \gamma(r, \pi - \theta) \tag{12}$$

and $\gamma(r, \theta)$ is completely determined once it is known in the angular range defined by $\varphi = 0$ and $0 \le \theta \le \pi/2$.

Equation (9) is an example of the oriented stick probability functions (oSPFs) discussed by Ciccariello (1985). Equation (III.4) of that paper gives the integral expression of the second derivative of any oSPF evaluated along two arbitrary directions $\hat{\boldsymbol{\mu}}$ and $\hat{\boldsymbol{\nu}}$. Thus, applying this formula to (9) and setting $\hat{\boldsymbol{\mu}} = \hat{\boldsymbol{\nu}} = \hat{\boldsymbol{\omega}}$, the integral expression of the second partial derivative of $\gamma_W(\mathbf{r})$ with respect to r will be

$$V_p\gamma''_W(r\hat{\boldsymbol{\omega}}) = -\int_S (\mathrm{d}\mathbf{S}_1\cdot\hat{\boldsymbol{\omega}})\int_S (\mathrm{d}\mathbf{S}_2\cdot\hat{\boldsymbol{\omega}})\delta(\mathbf{r}_1 + r\hat{\boldsymbol{\omega}} - \mathbf{r}_2). \tag{13}$$

Here, $\mathrm{d}\mathbf{S}_i$ ($i = 1, 2$) is a vector set at point $\mathbf{r}_i$ of the particle boundary S, orthogonal to the latter, pointing externally to the particle and having length equal to the infinitesimal surface element $\mathrm{d}S_i$. δ represents the Dirac function. The latter implies that the only points belonging to Γ, the curve intersection of the boundaries of the fixed and of the translated spherical segment, contribute to the integral. Γ does not exist when $r > 2\sin\alpha = AC$ (see Fig. 1). Thus,

$$\gamma''(r, \theta) = 0 \quad \text{when} \quad r > 2\sin\alpha. \tag{14}$$

At smaller r, two Γ configurations are possible, depending on whether A_t, the point obtained translating A by $\mathbf{r}$, lies outside or inside the fixed spherical segment. In the first case (I), Γ is a parallel of the fixed spherical segment because it results from the intersection of the basis (*i.e.* the planar part) of the translated spherical segment with the round part of the fixed spherical segment. In the second case (II), Γ has the shape shown in Fig. 1 and comprises the arcs $\Gamma_1 = P_1P_2P_3$ and $\Gamma_2 = P_3PP_1$. Let $\bar{S}$ denote the point intersection of the circle of radius r centered at A with the arc AVC and let $\theta_0(r)$ denote the angle formed by axis z' with the half-line $A\bar{S}$. Clearly,

$$\theta_0(r) = \pi/2 - \alpha + \arcsin(r/2), \tag{15}$$

and configurations I and II occur when

$$\text{I} \quad 0 \le \theta \le \theta_0(r) \quad \text{and} \quad r \le 2\sin(\alpha/2) \tag{16a}$$

$$\text{II} \quad \theta_0(r) \le \theta \le \pi/2 \quad \text{and} \quad r \le 2\sin\alpha. \tag{16b}$$

[Note that in case I the existence of Γ requires a smaller range of distances because the basis of the translated spherical segment lies above the fixed

* The details of some algebraic manipulations are reported in Appendices *A*, *B* and *C*, which have been deposited with the British Library Document Supply Centre as Supplementary Publication No. SUP 71055 (10 pp.). Copies may be obtained through The Technical Editor, International Union of Crystallography, 5 Abbey Square, Chester CH1 2HU, England. It is also emphasized that Appendix *B* corrects a wrong statement by Ciccariello (1985). In Appendix *B*, it is shown that, for the second derivative to have a finite discontinuity, the parallelism of the surface and of its translated image at a point is sufficient, while, contrary to the statement made by Ciccariello (1985), the orthogonality of the tangent plane to the translation vector is by no means required. The latter condition is necessary only for the discontinuity to survive in the second derivative of the SAXS correlation function. In fact, the angular average over all reflection directions in general washes out such a discontinuity, unless the locally parallel surfaces are orthogonal to the translation.

spherical segment when $2\sin(\alpha/2) \le r \le 2\sin\alpha$.] The evaluation of integral (13) in cases I and II is explained in detail in Appendix *A*.* After

$$d_I(r,\theta) \equiv r\cos\theta + \cos\alpha, \tag{17a}$$

$$D(r,\theta) \equiv \cos\alpha + (r/2)\cos\theta, \tag{17b}$$

$$d_1(r,\theta) \equiv (r/2)\sin\theta - D(r,\theta)\cot\theta, \tag{17c}$$

$$d_2(r,\theta) \equiv D(r,\theta)/\sin\theta, \tag{17d}$$

$$R_1(r,\theta) \equiv [1 - d_I^2(r,\theta)]^{1/2}, \tag{17e}$$

$$R_2(r) \equiv [1 - (r/2)^2]^{1/2}, \tag{17f}$$

and

$$\phi_1(r,\theta) \equiv \arccos[d_1(r,\theta)/R_1(r,\theta)], \tag{17g}$$

$$\phi_2(r,\theta) \equiv \arccos[d_2(r,\theta)/R_2(r)], \tag{17h}$$

have been set, the final expressions for $\gamma''(r,\theta)$ in cases I and II, respectively, are

$$V_p\gamma_I''(r,\theta) = 2\pi\cos^2\theta(\cos\alpha + r\cos\theta), \tag{18a}$$

$$\begin{aligned} V_p\gamma_{II}''(r,\theta) &= [2d_1\phi_1\cos^2\theta + 2R_1(\sin\theta)(\cos\theta)(\sin\phi_1)] \\ &\quad + [(r/2)\phi_2] \\ &\equiv G_1(r,\theta) + G_2(r,\theta). \end{aligned} \tag{18b}$$

Here, V_p denotes the spherical segment volume given by

$$V_p = \pi\{1 - \cos\alpha - [(1 - \cos^3\alpha)/3]\}. \tag{19}$$

The taper parameter L and the rotundity parameter M, introduced respectively by Wilson (1962) and by Mitra (1964) [see also Wilson (1971)], are defined as $L = V_p^{2/3}\gamma''(0^+,\theta)$ and $M = -V_p\gamma'''(0^+,\theta)$. Using (18), in case I ($0 \le \theta \le \pi/2 - \alpha$) and case II ($\pi/2 - \alpha \le \theta \le \pi/2$), one obtains

$$L_I = V_p^{-1/3}2\pi(\cos\alpha)\cos^2\theta, \tag{19a}$$

$$\begin{aligned} L_{II} &= 2V_p^{-1/3}(\cos\theta)[(\sin^2\alpha - \cos^2\theta)^{1/2} \\ &\quad + (\cos\alpha)(\cos\theta)\arccos(-\cot\alpha/\cot\theta)], \end{aligned} \tag{19b}$$

$$M_I = -2\pi\cos^3\theta \tag{20a}$$

and

$$\begin{aligned} M_{II} &= -2(\cos^2\theta)\{(\cos\theta)\arccos(-\cot\alpha/\cot\theta) \\ &\quad - [(\cos\alpha)(\sin^2\alpha - \cos^2\theta)^{1/2}/\sin^2\alpha]\} \\ &\quad - (1/2)\arccos[(\cos\alpha)/(\sin\theta)]. \end{aligned} \tag{20b}$$

Fig. 2 shows the behavior of these quantities for some values of α. [Note that the taper-parameter expression, obtained by Wilson (1969) for a hemisphere, is immediately recovered if one sets $\alpha = \pi/2$ in (19*b*).] Although (18) could be explicitly integrated in order to obtain the WAXS correlation function, in practice it is more convenient to know the peak profiles that can be directly obtained by (18). In fact, the peak profile around the reflection characterized by the polar angle θ is

$$\begin{aligned} I_\theta(h) &= CV_p\int_0^\infty \cos(hr)\gamma(r,\theta)\,dr \\ &= (C/h^2)[S(\theta) - V_p\int_0^\infty \cos(hr)\gamma''(r,\theta)\,dr]. \end{aligned} \tag{21}$$

[The last equality follows the performance of two partial integrations and the use of the result (Wilson, 1949) that $\gamma'(0^+,\theta) = -S(\theta)/V_p$, where $S(\theta)$ is the area of the projection of the particle surface on a plane orthogonal to the reflection direction. C is a normalization constant such that $I_\theta(0) = 1$.] Fig. 3 shows the peak profiles and their Porod plots (Ciccariello, 1990) for some θ's. Details of the determination of $S(\theta)$ and the evaluation of (21) as well as a brief discussion of some features of the curves shown in Fig. 3 can be found in Appendix *B*.*

III. Edge contribution

The spherical-segment edge sharpness $\mathscr{S}$ will now be evaluated. By definition (3), $\mathscr{K}$ turns out to be given by

$$\mathscr{K} = \pi(1 - \cos\alpha), \tag{22}$$

* See deposition footnote.

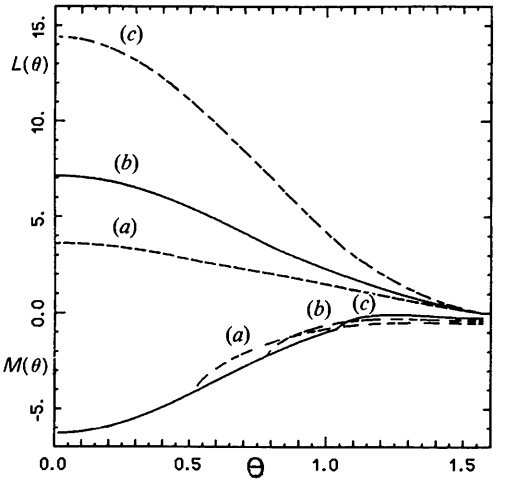

Fig. 2. The upper and lower sets of curves show the dependences of the taper and rotundity parameters, respectively, of the spherical segments on the reflection direction θ. Curves (*a*), (*b*) and (*c*) of each set are characterized by the opening angles: $\alpha = \pi/3$, $\pi/4$ and $\pi/6$, respectively. The decrease of the taper parameter with increasing α is evident. The rotundity curves shown coincide in the θ range where (20*a*) holds true. Their shape, however, is such that their angular averages yield the same value as given by (24).

* See deposition footnote.

while $\gamma'''(0)$ can be evaluated from (18). In fact, from (8) and (9),

$$\gamma''(r) = (4\pi)^{-1}\int \gamma''(r,\theta)\,\mathrm{d}\hat{\omega}$$
$$= \int_0^{\theta_0(r)} \sin\theta\,\gamma_{\mathrm{I}}''(r,\theta)\,\mathrm{d}\theta + \int_{\theta_0(r)}^{\pi/2} \sin\theta\,\gamma_{\mathrm{II}}''(r,\theta)\,\mathrm{d}\theta.$$

Thus,

$$\gamma'''(0^+) = \lim_{r\to 0^+}\Bigg(\int_0^{\theta_0(r)} \sin\theta\,\gamma_{\mathrm{I}}'''(r,\theta)\,\mathrm{d}\theta + \int_{\theta_0(r)}^{\pi/2} \sin\theta\,\gamma_{\mathrm{II}}'''(r,\theta)\,\mathrm{d}\theta + \theta_0'(r)\sin\theta_0(r)\{\gamma_{\mathrm{I}}''[r,\theta_0(r)] - \gamma_{\mathrm{II}}''[r,\theta_0(r)]\}\Bigg).$$

The term inside the curly brackets vanishes because $\gamma_{\mathrm{I}}'[r,\theta_0(r)]$ continuously matches $\gamma_{\mathrm{II}}'[r,\theta_0(r)]$. In the limit $r\to 0$, it gives $\theta_0(r)\to \pi/2-\alpha$ and

$$\gamma'''(0^+) = \int_0^{\pi/2-\alpha} \sin\theta\,\gamma_{\mathrm{I}}'''(0^+,\theta)\,\mathrm{d}\theta + \int_{\pi/2-\alpha}^{\pi/2} \sin\theta\,\gamma_{\mathrm{II}}'''(0^+,\theta)\,\mathrm{d}\theta. \quad (23)$$

The evaluation of the first integral is trivial. That of the second requires quite a lot of algebra owing to the derivative's involved expression. The details are reported in Appendix *C*.* The final result is quite simple:

$$4V_p\gamma'''(0^+) = 2\pi. \quad (24)$$

Though the volume of the generic spherical segment, given by (19), depends on α, it is remarkable that the r.h.s. of (31) is independent of α. Thus, the *roundedness* of a spherical segment is equal to that of the complete sphere. Comparing (24) with (22) and recalling (5), one obtains the *sharpness* of a spherical segment:

$$\mathscr{S}(\alpha) = \pi(1+\cos\alpha). \quad (25)$$

This quantity, in contrast to cases of truncated circular right cones (Ciccariello, 1993) and of right prisms (Sobry *et al.*, 1991), is always positive. Moreover, in contrast to cases of right cylinders, it does not vanish when the dihedral angle α is equal to $\pi/2$. Therefore, it appears reasonable that the sharpness, in general, will depend on both the dihedral angle and the Gaussian and squared mean curvatures of the surfaces on the edge of intersection. It is hoped that the former results may give a hint when the unknown general integral expression for $\mathscr{S}$ is sought. In any case, the positiveness of (25) shows that $\mathscr{S}$ does not yield an upper bound of the exact $\gamma'''(0)$ value.

Finally, the aforesaid evaluation of the second derivative of the WAXS correlation function, *i.e.* (9), can be performed also in the case of a spherical segment characterized by an opening angle α larger than $\pi/2$, although more angular ranges must be considered when r is not very small. However, when $r\simeq 0$, it is rather simple to show that the sharpness is still given by (25), which, in fact, yields a vanishing $\mathscr{S}$ for $\alpha=\pi$.

The author is grateful to Mr A. Rampazzo for kindly having drawn Fig. 1. Financial support from MURST through 40% and 60% Funds is also acknowledged.

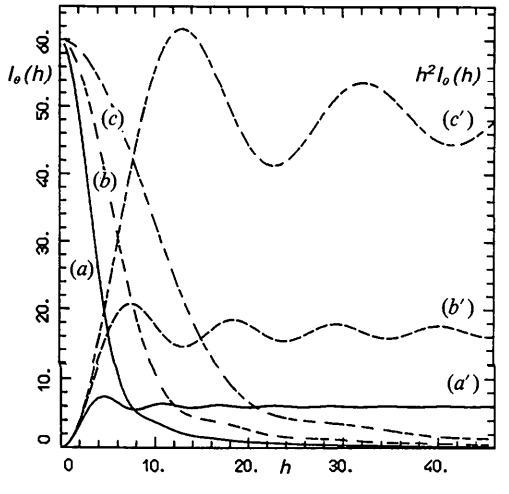

Fig. 3. Curves (*a*), (*b*) and (*c*) are the peak profiles (normalized to 60 for drawing convenience) of the spherical segment, characterized by $\alpha=\pi/4$, along the directions $\theta=3\pi/7$, $\pi/3$ and $\pi/6$, respectively. (It is recalled that the distance unit is such that R, the spherical-segment radius, is equal to one, while h is in units R^{-1}.) Curves (*a'*), (*b'*) and (*c'*) give the corresponding Porod plots, *i.e.* $h^2I_\theta(h)$ *versus* h. [Note that these curves refer to the normalization $I_\theta(0)=1$.]

* See deposition footnote.

References

BRUMBERGER, H., GOODISMAN, J. & RAMAYA, R. (1990). International Conference on Small-Angle X-ray Scattering, Leuven, Belgium.

CICCARIELLO, S. (1985). *Acta Cryst.* **A41**, 560–568.

CICCARIELLO, S. (1990). *Acta Cryst.* **A46**, 175–186.

CICCARIELLO, S. (1993). *Acta Cryst.* **A49**, 398–405.

CICCARIELLO, S., GOODISMAN, J. & BRUMBERGER, H. (1988). *J. Appl. Cryst.* **21**, 117–128.

DEBYE, P., ANDERSON, H. R. & BRUMBERGER, H. (1957). *J. Appl. Phys.* **28**, 679–683.

KIRSTE, R. & POROD, G. (1962). *Kolloid Z.* **184**, 1–7.

MÉRING, J. & TCHOUBAR, D. (1968). *J. Appl. Cryst.* **1**, 153–165.
MITRA, B. G. (1964). *Br. J. Appl. Phys.* **15**, 917–921.
POROD, G. (1951). *Kolloid Z.* **124**, 83–87; **125**, 51–56.
POROD, G. (1982). In *Small-Angle X-ray Scattering*, edited by O. GLATTER & O. KRATKY, ch. 1. London: Academic Press.
ROWLINSON, J. S. & WIDOM, B. (1982). *Molecular Theory of Capillarity*, § 1.3. Oxford: Clarendon Press.
SOBRY, R., LEDENT, J. & FONTAINE, F. (1991). *J. Appl. Cryst.* **24**, 516–525.
STOKER, J. J. (1989). *Differential Geometry*. New York: Wiley.
WILSON, A. J. C. (1949). *X-ray Optics*. London: Methuen.
WILSON, A. J. C. (1962). *Proc. Phys. Soc. London*, **80**, 286–294.
WILSON, A. J. C. (1969). *J. Appl. Cryst.* **2**, 181–183.
WILSON, A. J. C. (1971). *J. Appl. Cryst.* **4**, 440–443.

Acta Cryst. (1993). A**49**, 755–762

The Measurement of Defect Parameters in Imperfect Crystals using X-ray Diffraction

BY T. J. DAVIS

CSIRO Division of Materials Science and Technology, Private Bag 33, *Rosebank MDC, Clayton, Victoria* 3169, *Australia*

(*Received* 27 *January* 1993; *accepted* 5 *April* 1993)

Abstract

Correlation lengths and defect-strength parameters, related to the separations and magnitudes of discontinuities in imperfect crystals, are obtained from X-ray rocking curves using a stochastic model of crystal defects. The model describes the diffraction of X-rays from an imperfect crystal containing surfaces of defects, such as stacking faults, and misoriented crystal grains. The two defect parameters provide a measure of crystal quality. A method of extracting the parameters from rocking curves is described in the limit of kinematic X-ray diffraction. The method is applied to X-ray diffraction data obtained from thin films of CdTe and $Hg_{1-x}Cd_xTe$ grown on GaAs substrates. The ability of the model to fit the X-ray data is a test of the stochastic model.

Introduction

X-ray diffraction is used extensively to measure the quality of thin crystalline films grown by techniques such as molecular-beam epitaxy and metalorganic chemical vapour deposition. A single parameter, the full width at half-maximum of the Bragg reflection, is the usual measure of the crystal quality. However, many theories of X-ray diffraction from imperfect crystals involve two parameters related to the nature of the imperfections (Zachariasen, 1967; Kato, 1980; Becker & Al Haddad, 1990; Davis, 1992). Therefore, it should be possible to obtain a better measure of the crystal quality by extracting two parameters from the X-ray data.

The stochastic model of X-ray diffraction developed by Davis (1992) describes the mean reflectivity from an imperfect extended-face crystal containing surfaces of defects and misoriented crystal grains. These defects produce discontinuities in the strain and strain gradients in the crystal. The model contains two parameters: a defect-'strength' parameter, σ, and a correlation length, l. The correlation length is defined by a correlation function and is the distance over which the correlation between the phases of the diffracted X-rays falls by $1/e$. If the width of the Bragg reflection, related to $\nu^2 = \sigma^2/2l$, is chosen as one independent measure of the crystal quality, then a possible choice for the second independent parameter is the correlation length.

The aim of this paper is to verify that the stochastic model can fit X-ray data from a number of thin films and to demonstrate the method by which the two defect parameters may be obtained. The model is applied in a kinematic limit to X-ray data sets obtained from thin films of CdTe and $Hg_{1-x}Cd_xTe$ grown on GaAs substrates. In the following sections, the stochastic model is briefly reviewed, the method for fitting the model to the data is described and the experiments and their results are discussed.

Theory

The stochastic defect model for X-ray diffraction from imperfect crystals is based on a form of the Takagi–Taupin equations (Takagi, 1962, 1969; Taupin, 1964). The main aspects of this model are summarized below. For a complete description of the model the reader is referred to Davis (1992).

For thin films in which the change in the amplitude of the transmitted wave is small, a *kinematic* solution for the complex reflectance $R(t)$ at depth t is

$$R(t) = \exp[-i2\alpha\int_0^t \beta(t')\,dt']\int_0^t i\alpha\chi_h(t') \times \exp[i2\alpha\int_0^{t'} \beta(t'')\,dt'']\,dt', \quad (1)$$

ISSN 0108-7673